Copyright Notice

Institute of Communication Networks and Computer Engineering
University of Stuttgart
Pfaffenwaldring 47, D-70569 Stuttgart, Germany
Phone: ++49-711-685-68026, Fax: ++49-711-685-67983
email: mail@ikr.uni-stuttgart.de, http://www.ikr.uni-stuttgart.de

Local Interference Coordination in Cellular OFDMA Networks

Marc C. Necker
Institute of Communication Networks and Computer Engineering, University of Stuttgart
Pfaffenwaldring 47, D-70569 Stuttgart, Germany
Email: marc.necker@ikr.uni-stuttgart.de

***Abstract*— Orthogonal Frequency Division Multiple Access (OFDMA) is a promising concept, which is the basis of the currently emerging 802.16e (WiMax) and 3GPP Long Term Evolution (LTE) cellular systems. OFDMA is basically a combination of FDM and TDM, and therefore suffers from heavy inter-cell interference if neighboring basestations use the same frequency range. However, it is desirable to reuse the complete available frequency spectrum in every cell in order to maximize the resource utilization. One approach to solve this conflict is the application of beamforming antennas in combination with interference coordination mechanisms between basestations. Starting from a global interference coordination scheme with full system knowledge, we investigate how spatially limited interference coordination affects the system performance. Subsequently, we study several realizable interference coordination schemes and show that a locally implementable scheme can almost match the performance of the global scheme with respect to the sector throughput.**

I. Introduction

Several emerging standards for broadband cellular communication are based on OFDMA. In particular, 802.16e (mobile WiMax) and future 3GPP Long Term Evolution (3GPP LTE) cellular systems will offer high-speed packet switched services for a variety of applications. In OFDMA, users are multiplexed in time and frequency based on the underlying OFDM system, which basically corresponds to a combination of Frequency and Time Division Multiplexing (FDM and TDM). A major problem in FDM/TDM systems is the inter-cell interference that neighboring cells create when using the same frequency band. Classical FDM/TDM systems like GSM mitigate inter-cell interference by avoiding the reuse of the same set of frequencies in neighboring cells by employing a frequency reuse pattern. Another possibility is to use beamforming antennas, which focus their transmission or reception in the direction of a particular terminal. This minimizes the interference to terminals in other directions. Finally, the transmissions of neighboring base-stations can further be coordinated, thus almost completely eliminating inter-cell interference [1]. This is referred to as interference coordination (IFCO).

IFCO is gaining more and more attention in the course of 3GPP LTE and 802.16e, as it seems the most promising approach to solve the problem of inter-cell interference in OFDMA-systems while achieving a high spectral efficiency at the same time. Besides a solid network and protocol architecture to allow the realization of IFCO, intelligent algorithms to coordinate the transmissions to different terminals are needed.

In [2], the application of beamforming antennas in 802.16e for spatial multiplexing of concurrent transmissions within a cell sector is considered. This is done in combination with a local coordination scheme at the basestation while focusing on the avoidance of intra-cell interference. The case of inter-cellular coordination in order to reduce interference is studied in [3] and [4], however without directly taking into account beamforming antennas. In both papers, the authors focus on a flow-level analysis of the possible capacity gains with inter-cellular coordination in some basic scenarios. They derive the optimal boundaries of regions which may or may not be served by the same basestations at the same time, resulting in a static scheduling policy for each cell.

In [1], we investigated a global interference coordination scheme with beamforming antennas and full system knowledge in a dynamic 802.16e-system. Despite the fact that such a global scheme is not realizable, it provides an important reference for future distributed solutions. Based on the scheme presented in [1], we study in this paper the impact of limited coordination between basestations as it would be the case in an actual system. We subsequently introduce several IFCO algorithms which are implementable locally within a basestation and compare their performance to the global scheme. We finally propose a local algorithm with almost the same overall spectral efficiency as the global scheme.

This paper is structured as follows. In section II, the investigated 802.16e-system is introduced. Section III details the considered IFCO algorithms, and section IV presents the performance evaluation. Finally, section V concludes the paper.

II. System model

A. Overview of transmission system

We consider an 802.16e-system [5] with a total available system bandwidth of 10 MHz and a MAC-frame-length of 5 ms. This results in a total number of 49 OFDM-symbols per MAC-frame and 768 data subcarriers per OFDM-symbol. Each MAC-frame is subdivided into an uplink and a downlink subframe. Both subframes are further divided into zones, allowing for different operational modes. In this paper, we focus on the Adaptive Modulation and Coding (AMC) zone in the downlink subframe. In particular, we consider the AMC 2x3 mode, which defines subchannels of 16 data subcarriers by 3 OFDM-symbols. This is illustrated in the left part of Fig. 1. A subchannel corresponds to the resource assignment granularity for a particular mobile terminal. The AMC zone can therefore be abstracted by the two-dimensional resource field shown in the right part of Fig. 1.

We assume the AMC zone to consist of 9 OFDM-symbols, corresponding to a total number of $48 \cdot 3$ available subchannels. Adaptive Modulation and Coding was applied ranging from QPSK 1/2 up to 64QAM 3/4. This results in a theoretical maximum raw data rate of about 6.2 Mbps within the AMC zone. The burst profile management is based on the exponential average of the SINR conditions of the terminal's previous data receptions.

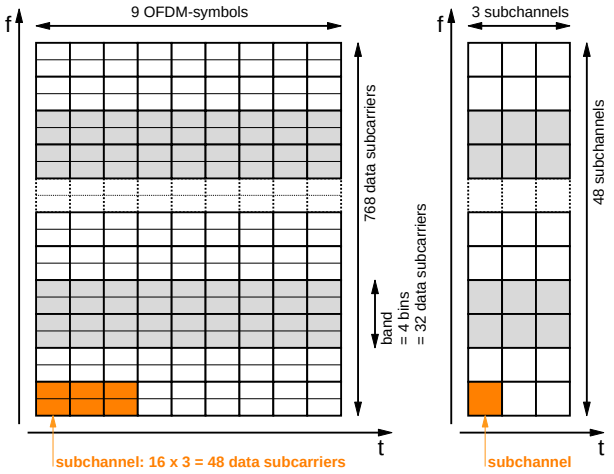

Fig. 1: Illustration of the AMC 2x3 mode

B. Simulation model

We consider a hexagonal cell layout comprising 19 basestations at a distance of $d_{\mathrm{BS}} = 1400$ m with 120° cell sectors as shown in Fig. 2. The scenario is simulated with wrap-around, making all cells equal with no distinct center cell. Throughout our paper, we evaluate the shaded *observation area* when investigating the cell coverage, and the average of all cell sectors when considering throughput metrics. All cells were assumed to be synchronized on a frame level. Each sector contains $N = 9$ fully mobile terminals moving at a velocity of 30 km/h, which are restricted to their respective cell sector in order to avoid handovers (see [1] for more details).

Every basestation has 3 transceivers, each serving one cell sector. The transceivers are equipped with linear array beamforming antennas with 4 elements and gain patterns according to [1]. They can be steered towards each terminal with an accuracy of 1° degree, and all terminals can be tracked ideally.

III. Interference Coordination and Resource Assignment

A. General procedure

In order to realize the coordination of cell sectors, we divide the scheduling and resource assignment process into two steps, which are performed for each MAC frame:

1) *Interference coordination:* In this step, the resources available for each mobile terminal are restricted according to a certain algorithm. By doing so, it can be avoided that certain mobile terminals in different cells are served on the same set of resources (see section III-B).
2) *Resource assignment:* In this second step, a scheduler assigns resources to the different terminals, while taking into account the constraints of the previous step. This is detailed in section III-D.

Note that it depends on the respective interference coordination mechanism whether a distributed or even a local implementation of these two steps may be feasible or not.

In the following, we consider the graph based interference coordination algorithm from [1] and the concept of Fractional Frequency Reuse (FFR), including several variants and combinations thereof. Section III-B summarizes the global interference coordination scheme from [1]. Section III-C introduces FFR and the considered variants. Finally, section III-D details the resource assignment procedure.

B. Interference Coordination with Interference Graph

This scheme from [1] is based on an interference graph whose nodes represent the mobile terminals, and whose edges represent critical interference relations in-between the terminals. Terminals which are connected must not be served using the same set of resources. For each terminal, the interference from basestations within a certain diameter d_{ic} of the serving basestation is calculated. Afterwards, the largest interferers are blocked from using the same set of resources by establishing a relation in the interference graph. This is done such that a desired minimum SIR D_S is achieved for each terminal. For a detailed description, please refer to [1].

The coordination diameter d_{ic} denotes the maximum distance which two basestations may have in order to still be coordinated. The larger the coordination diameter, the more challenging is an implementation in a real system. In [1], d_{ic} was infinite, which implies a global interference coordination with an omniscient device capable of instantly acquiring the system state and assigning the resources on a per-frame basis. This is an ideal solution, which is not feasible in an actual system, but it provides some important performance metrics for the comparison of realizable algorithms.

Limiting d_{ic} to the distance d_{BS} between two basestations restricts the coordination to neighboring basestations. This coordination with a diameter of one tier (one-tier coordination) requires signaling only between neighboring basestations giving way to a possible distributed realization of the interference coordination. Further decreasing d_{ic} leads to a coordination only among the sectors of the same basestation (zero-tier coordination). Such a scheme was proposed in [6]. It can be implemented locally within a basestation and does not need

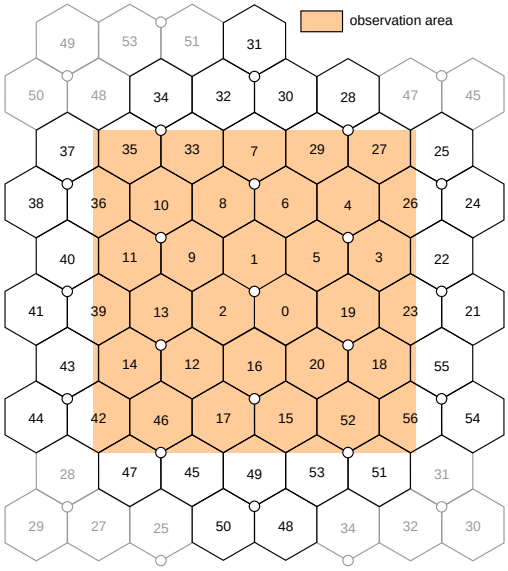

Fig. 2: Hexagonal cell layout with wrap-around

any signaling among basestations.

C. Fractional Frequency Reuse (FFR)

FFR is a well-known concept to mitigate inter-cell interference without the need for global coordination. It is based on the idea of applying a frequency reuse of one in areas close to the basestation, and a higher reuse in areas closer to the cell border. This idea was first proposed for GSM networks (see for example [7]) and has consequently been adopted in the WiMAX forum [8], but also in the course of the 3GPP Long Term Evolution (LTE) standardization, e.g., in [9] and [10], where the focus lies on practically implementable algorithms.

Several variations of such a scheme are possible. In [6], the reuse 1 and reuse 3 areas are on disjoint frequency bands, while [9] and [10] use the full set of available resources in the reuse 1 areas and one third of the same resources in the reuse 3 areas. This difference is illustrated in Fig. 3. Variations are also possible with respect to the transmit power level in each of the areas. In [9], the reuse 1 areas are covered with a reduced power level, while in [10] the transmit power of interfering base stations is reduced. In this paper, we will use the full set of resources for the reuse 1 areas and one third of the same resources for the mobiles in the reuse 3 areas (Fig. 3 top). The power will not be controlled as part of the interference coordination, but in the course of the burst profile management.

The assignment of mobile terminals to reuse 1 or reuse 3 areas can be done based on the distance d_{MT} of a mobile terminal from the basestation [6], or on the present SINR situation. In this paper, we consider both possibilities. For the distance-based assignment, a distance ratio $d_{13} = 2d_{\mathrm{MT}}/d_{\mathrm{BS}}$ is introduced. If $d_{\mathrm{MT}} < d_{13}$, the mobile terminal is served in the reuse 1 area, otherwise it is served in the reuse 3 area.

The SINR-based assignment can be done based on measurements in the mobile terminal. These may be based on the measurement of pilots from the serving and the interfering basestations, or on measurements of recently received data frames. The measurements need to be fed back to the basestation, which is also required for other purposes, such as burst profile selection. In the following, we will only consider measurements on actually received data frames. To take into account the high variability of the instantaneous SINR, the decision regarding the reuse 1 or reuse 3 area is based on a hysteresis. This is done by introducing an upper SINR threshold th_{up} and a lower SINR threshold th_{low}, as illustrated in Fig. 4. Instead of the instantaneous SINR, an exponential average of the previously experienced SINR-values of each mobile terminal is used, which reflects the averaged SINR conditions the mobile terminal is currently experiencing.

FFR can be combined with an additional interference coordination algorithm. In [6], it was proposed to coordinate the transmissions within the sectors of one basestation on top of the distance-based FFR scheme, while the coordination algorithm was described only on a high level. In the following, we propose to combine the distance- and SINR-based FFR with the interference graph based coordination scheme described in the previous section. We will limit the interference graph based algorithm to just local coordination in-between sectors of the same basestation (zero-tier coordination), in order to preserve the possibility of a local implementation. We will show that FFR in combination with the additional local interference coordination greatly outperforms a pure FFR scheme with no coordination.

Note that in contrast to classical Dynamic Channel Assignment (DCA) schemes, in particular Autonomous Reuse Partitioning (ARP) (see for example [11] for a good overview), the here investigated FFR schemes are much more dynamic and act on a per-frame basis. They additionally utilize the benefits of beamforming antennas and local interference coordination.

D. Resource Assignment

In each cell sector, a Random scheduling mechanism is used, which assigns the highest scheduling priority to each of the N mobile terminals in a cell sector at least once within a period of N MAC-frames. For each MAC frame, the resource assignment process begins by randomly selecting a cell sector and assigning a rectangle of 3×12 subchannels to the highest priority terminal m_k. If an interference graph is used for interference coordination, the assigned resources are blocked for all other terminals connected to m_k in the interference graph. Afterwards, another cell sector is randomly selected and the highest priority terminal is assigned resources, obeying possible resource blockings. Once all sectors have been visited, the whole procedure is repeated with the second highest priority terminals, and so on.

IV. Performance Evaluation

A. Scenario and simulation parameters

The system model was implemented as a frame-level simulator using the event-driven simulation library IKR SimLib [12]. The path loss was modeled according to [13], terrain category B. Slow fading was considered using log-normal shadowing with standard deviation 8 dB. Frame errors were modeled based on BLER-curves obtained from physical layer simulations. The simulation model comprised all relevant protocols, such as fragmentation, ARQ and

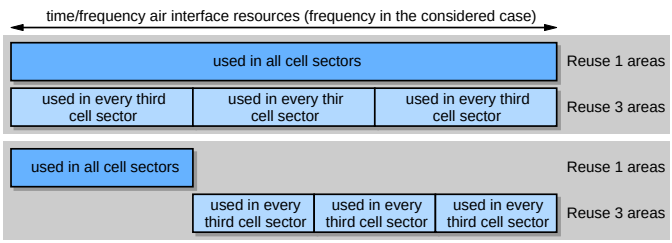

Fig. 3: Schematic illustration of FFR with the same (top) and disjoint (bottom) resources for reuse 1 and reuse 3 areas.

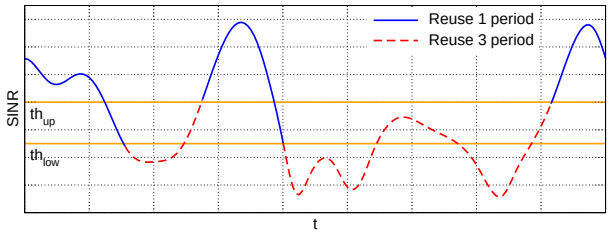

Fig. 4: Selection of reuse area based on SINR

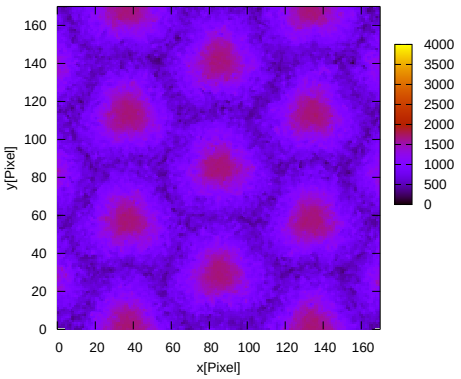

Fig. 5: Frequency Reuse 3: Mean throughput [kBit/s] in observation area

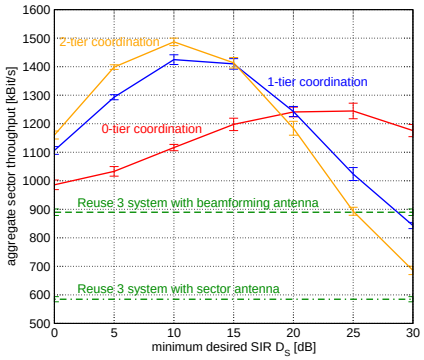

Fig. 6: Interference graph based IFCO: Total sector throughput over D_S

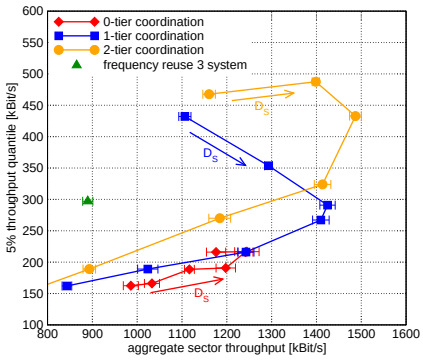

Fig. 7: Interf. graph based IFCO: 5% throughput quantile over total throughput

HARQ with chase combining. All results were obtained for the downlink direction with greedy traffic sources. Throughput measurements were done on the IP-layer, capturing all effects of SINR-variations and retransmissions. This also captures the overhead of MAC protocol headers and padding of the 64-Byte ARQ blocks when packing them into bursts.

B. Interference coordination based on interference graph

This scheme was studied extensively in [1] assuming a global omniscient device. In the following, we consider the influence of the coordination diameter as introduced in section III-B, which is a first step towards a distributed implementation. As a reference, Fig. 5 shows the average achievable throughput over the observation area as defined in Fig. 2 for a classical frequency reuse 3 system with beamforming antennas. The mean sector throughput is about 890 kBit/s, corresponding to a spectral efficiency of almost 0.5 Bit/Hz/s, which is an increase of about 50% over a reuse 3 system with sector antennas. In this scenario, the obtained throughput in the center of the cell is about 2—3 times higher than in the cell border areas.

The total sector throughput for the interference coordinated Reuse 1 system is shown in Fig. 6, for different diameters d_{ic}. As we increase D_S, the SIR conditions improve, while on the other hand the resource utilization decreases due to an increased number of interference graph conflicts. This leads to a tradeoff and a maximum of the observed total sector throughput for a particular D_S. This effect was studied in [1], and will also be illustrated in section IV-C for the distance-base FFR.

With respect to the coordination diameter, the total sector throughput decreases as d_{ic} is decreased. For smaller d_{ic}, it is more difficult to control the interference situation in the border areas of the cell sectors, and it is no longer possible to achieve uniform SIR averages in the area as those observed in [1] with global interference coordination. Consequently, larger values of D_S are required to compensate this effect and achieve the maximum sector throughput. In all cases, the maximum achieved sector throughput is higher than in the reuse 3 system.

Besides the total sector throughput, fairness is an important issue. In particular, terminals which are far away from the basestation should still receive an acceptable service. The 5% throughput quantile is a good indication for the achievable throughput in the cell border areas [14]. Here, it is captured by measuring the average short-term throughput of each terminal within 4-second periods and calculating the quantile over all measurements. The 5% quantile is shown in Fig. 7 depending on the total sector throughput. The measurement points are spaced 5 dB apart and correspond to the values of D_S in Fig. 6. For a zero-tier coordination, the maximum sector throughput automatically delivers the best cell edge performance. For a larger coordination diameter the cell border performance can be traded off against the aggregate throughput. This is particular the case for the one-tier coordination. In contrast, the two-tier coordination has even more control over the SIR in the cell border areas and achieves an almost maximum throughput quantile and maximum aggregate throughput at the same time. Note that the throughput quantile decreases as the minimum desired SIR D_S increases, since more conflicts in the interference graph are introduced especially for mobile terminals in the cell border areas.

Figure 8 and 9 give even more insight by plotting the throughput in the observation area for the one-tier and the zero-tier coordinated system. The throughput improvement is mainly observed in the inner portion of the cell area, especially when comparing the results to the reuse 3 system in Fig. 5. The graphs also reveal the cell border areas where the throughput is particularly low. The throughput in the border areas could be improved by moving to a two-tier coordination, or by sacrificing aggregate sector throughput.

Note that a coordination of only neighboring basestations achieves an almost as high aggregate throughput as a coordination with a larger coordination diameter. Even the zero-tier coordination, which takes place within a basestation and therefore is well-feasible, achieves a performance gain of approximately 30% over the reuse 3 system. However, the zero-tier coordinated Reuse 1 system suffers from degradation in the cell border areas and cannot match the aggregate performance of the systems with a larger coordination diameter. One approach to solve this problem while still avoiding coordination in-between basestations is the usage of FFR.

C. Distance-based FFR

Figure 10 shows the utilization of resources and the median of the sector SIR depending on the distance ratio d_{13}. If d_{13} is increased, the cell area where a reuse of 3 is enforced becomes smaller and the utilization of resources increases. At

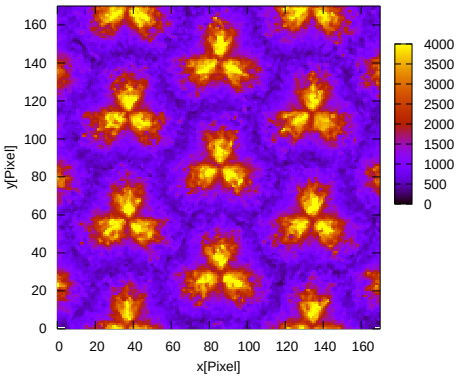

Fig. 8: Interference graph based IFCO: Mean throughput [kBit/s] for $D_S = 15$ dB and $d_{\mathrm{ic}} = 1$ (1-tier coordination)

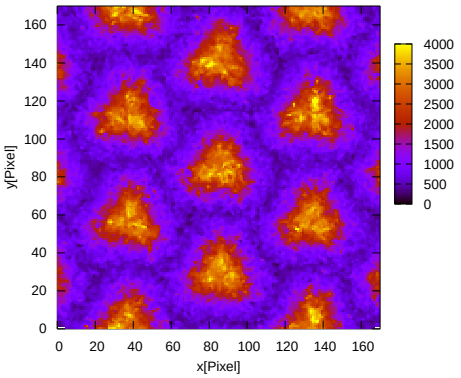

Fig. 9: Interference graph based IFCO: Mean throughput [kBit/s] for $D_S = 20$ dB and $d_{\mathrm{ic}} = 0$ (0-tier coordination)

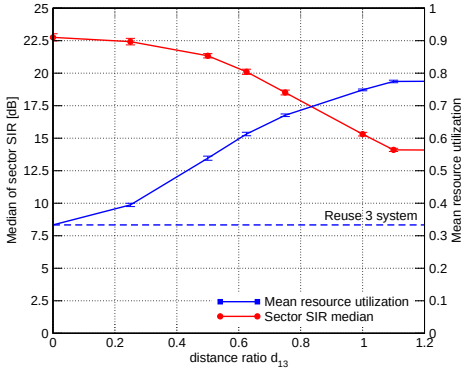

Fig. 10: Distance-based FFR with 0-tier coordination: Median of SIR and mean utilization of resources, $D_S = 20$ dB

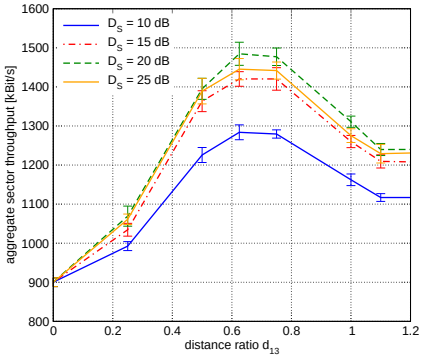

Fig. 11: Distance-based FFR with 0-tier coordination: Total sector throughput over d_{13} for different values of D_S

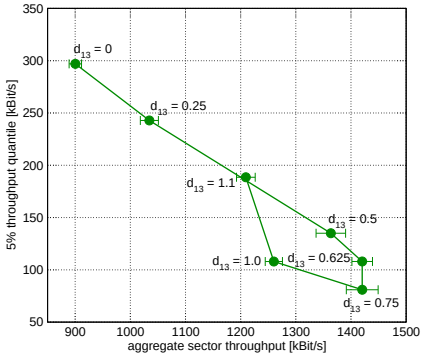

Fig. 12: Distance-based FFR: 5% throughput quantile depending on the total sector throughput, $D_S = 20$ dB

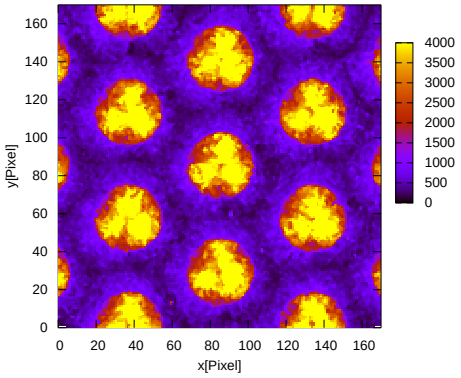

Fig. 13: Distance-based FFR: Mean throughput [kBit/s] in observation area for $d_{13} = 0.625$ and $D_S = 20$ dB

the same time, the median of the SIR decreases. Naturally, this will lead to a tradeoff. Figure 11 therefore shows the total sector throughput depending on d_{13} for different values of D_S. A desired SIR D_S of 20 dB delivers the best results. This is in line with the results of a pure interference graph based coordination in Fig. 6 for a coordination diameter of zero tiers. With respect to the distance ratio d_{13}, a value of about 0.6 delivers the best results, which nicely fits the results of [6].

Figure 12 plots the 5% throughput quantile over the total sector throughput for $D_S = 20$ dB. With respect to both the quantile and the total throughput, the performance of the interference graph based scheme with inter-cellular coordination cannot be met. The performance is rather comparable to the previously investigated zero-tier coordination scheme, where the additional FFR now allows to trade off the throughput quantile and the aggregate sector throughput. From the chart we can see that the aggregate throughput can be pushed to an almost as high throughput as in the globally coordinated system while sacrificing 50-70% of the cell border performance.

The area throughput in Fig. 13 reveals a sharp edge at the given distance ratio, where the throughput drops by a factor of 4–5. This is avoided by the SINR-based FFR which we evaluate in the following section.

D. SINR-based FFR

In this section, we consider two variants of the SINR-based fractional frequency reuse scheme: The pure SINR-based scheme without any coordination in-between cell sectors and basestations, and the same scheme with additional coordination among cell sectors of the same basestation based on the interference graph (zero tier coordination). In the uncoordinated case, the adjustable parameters are the lower and upper threshold th_{low} and th_{up}. In the coordinated case, D_S offers an additional degree of freedom.

As a first result, Fig. IV-C plots the average reuse factor which a mobile terminal experiences within the observation area in the coordinated case. As expected, the cell borders are covered with a reuse of 3, while large portions of the cell area are covered with an effective reuse of 1–2. A sharp edge as with the distance-based FFR is avoided.

Figure 15 plots the 5% throughput quantile over the total sector throughput for different SINR thresholds. All points of one curve represent different values of th_{low} and are spaced 5 dB apart with the first point representing $th_{\mathrm{low}} = 5$ dB and the last point $th_{\mathrm{low}} = th_{\mathrm{up}}$. Based on the previous results for zero tier coordination, D_S is set to 20 dB. From Fig. 15 we see that the uncoordinated system can obviously not match the performance of the coordinated system with respect to the aggregate throughput. In both cases, th_{up} and particularly

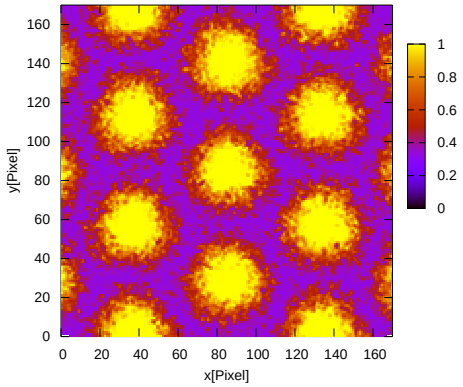

Fig. 14: SINR-based FFR with 0-tier coordination: Mean reuse factor, $D_S = 20$ dB, $th_{\text{up}} = 25$ dB, $th_{\text{low}} = 15$ dB

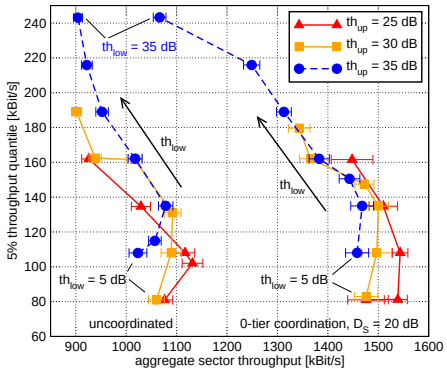

Fig. 15: SINR-based FFR: 5% quantile of sector throughput depending on total throughput, $D_S = 20$ dB

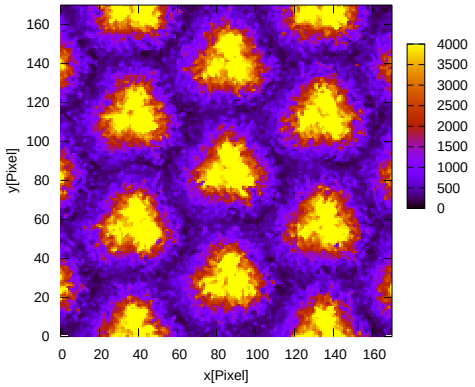

Fig. 16: SINR-based FFR with 0-tier coordination: Throughput [kBit/s], $th_{\text{up}} = 25$ dB, $th_{\text{up}} = 15$ dB

th_{low} allow to trade-off the aggregate throughput and the cell edge throughput.

The SINR-based FFR slightly outperforms the distance-based FFR with respect to both the aggregate throughput and the cell-edge throughput. Moreover, it has a soft degradation of the performance when moving from the cell center to the edge, avoiding a sharp edge as with the distance-based FFR. This is additionally illustrated in Fig. 16 by the throughput within the observation area. Summarizing the results, the performance of a system with inter-cellular coordination can almost be matched with regard to the total sector throughput. With respect to the cell border performance, the performance of the locally coordinated system is significantly worse, as inter-cellular coordination allows a much better control of the interference caused by neighboring basestations.

V. Conclusion

Interference coordination is essential in OFDMA-based cellular networks in order to achieve a high spectral efficiency and solve the problem of inter-cellular interference. We showed that coordination among neighboring base-stations almost matches the spectral efficiency of a global coordination. We further discussed several schemes based on FFR. It was shown that the aggregate sector throughput of a pure FFR scheme is only slightly better than that of a classical reuse 3 system. The performance can greatly be improved by additionally performing a local coordination in-between sectors of the same basestation to almost match the overall spectral efficiency of the global interference coordination scheme. The proposed SINR-based algorithm slightly outperforms the distance-based algorithm with respect to the overall spectral efficiency. It achieves about the same sector throughput as the global scheme while falling short with respect to the cell border performance. This results in a spectral efficiency of about 0.8 Bit/Hz/s for the locally coordinated reuse 1 system with FFR as compared to about 0.5 Bit/Hz/s for the reuse 3 system.

VI. Acknowledgments

This research was done in cooperation with Alcatel-Lucent Research and Innovation Department, Stuttgart.[1] The author would like to thank Bozo Cesar, Martin Link, Stephan Saur, Michael Scharf, and Andreas Weber for their valuable input.

References

[1] M. C. Necker, "Towards frequency reuse 1 cellular FDM/TDM systems," in *Proc. 9th ACM/IEEE International Symposium on Modeling, Analysis and Simulation of Wireless and Mobile Systems (MSWiM 2006)*, Torremolinos, Malaga, Spain, October 2006, pp. 338–346.

[2] C. Hoymann, H. Meng, and J. Ellenbeck, "Influence of SDMA-specific MAC scheduling on the performance of IEEE 802.16 networks," in *Proc. European Wireless (EW 2006)*, Athens, Greece, April 2006.

[3] T. Bonald, S. Borst, and A. Proutière, "Inter-cell scheduling in wireless data networks," in *Proc. European Wireless (EW 2005)*, Nicosia, Cyprus, April 2005.

[4] S. Liu and J. Virtamo, "Inter-cell coordination with inhomogeneous traffic distribution," in *Proc. 2nd Conference on Next Generation Internet Design and Engineering (NGI 06)*, València, Spain, April 2006.

[5] IEEE 802.16e, *IEEE Standard for Local and metropolitan area networks, Part 16: Air Interface for Fixed and Mobile Broadband Wireless Access Systems, Amendment 2: Physical and Medium Access Control Layers for Combined Fixed and Mobile Operation in Licensed Bands*, Aug. 2005.

[6] M. Sternad, T. Ottosson, A. Ahlen, and A. Svensson, "Attaining both coverage and high spectral efficiency with adaptive OFDM downlinks," in *Proc. 58th IEEE Vehicular Technology Conference (VTC 2003-Fall)*, vol. 4, October 2003, pp. 2486–2490.

[7] K. Begain, G. I. Rozsa, A. Pfening, and M. Telek, "Performance analysis of GSM networks with intelligent underlay-overlay," in *Proc. 7th International Symposium on Computers and Communications (ISCC 2002)*, Taormina, Italy, July 2002, pp. 135–141.

[8] "Mobile WiMAX – Part I: A technical overview and performance evaluation," WiMAX Forum, Tech. Rep., February 2006.

[9] 3GPP TSG RAN WG1#42 R1-050841, "Further analysis of soft frequency reuse scheme," Huawei, Tech. Rep., 2005.

[10] 3GPP TSG RAN WG1#42 R1-050764, "Inter-cell interference handling for E-UTRA," Ericsson, Tech. Rep., September 2005.

[11] H. Salgado, M. Sirbu, and J. Peha, "Spectrum sharing through dynamic channel assignment for open access to personal communications services," in *Proc. IEEE International Conference on Communications (ICC 1995)*, vol. 1, Seattle, WA, June 1995, pp. 417–422.

[12] *IKR Simulation Library*. [Online]. Available: http://www.ikr.uni-stuttgart.de/Content/IKRSimLib/

[13] V. Erceg, L. Greenstein, S. Tjandra, S. Parkoff, A. Gupta, B. Kulic, A. Julius, and R. Bianchi, "An empirically based path loss model for wireless channels in suburban environments," *IEEE Journal on Selected Areas in Communications*, vol. 17, no. 7, pp. 1205–1211, July 1999.

[14] 3GPP TS 25.814, *Physical layer aspects for evolved Universal Terrestrial Radio Access (UTRA) (Release 7)*, 3rd Generation Partnership Project, June 2006.

[1]Alcatel-Lucent Deutschland AG, Research & Innovation, Holderäckerstr. 35, 70435 Stuttgart, Germany. Contact: Michael Tangemann (Michael.Tangemann@alcatel-lucent.de).